Optical laser diffraction transducer for measuring single-wire electric cable eccentricity

M E Fedorov
National Research Tomsk Polytechnic University, 634028, Tomsk, Russia

E-mail: evgeny_fyodorov@list.ru

Abstract. The paper outlines some issues related to optical sensors based on the diffraction method which are used as a part of the devices to control the outer diameter and eccentricity of a single-core electric cable. The conversion function which allows calculation of the diameter of cylindrical objects regardless of their position in the tested area is considered. The calculations are based on the diffraction method to detect shadow boundaries of the object in two-dimensional optical sensors that use a divergent laser beam. The obtained results can be used to develop precise optical instruments to control the outer diameter and eccentricity of the object in a cable industry.

1. Introduction

In-process control of the diameter and eccentricity of the electric cable aims at solving the problem of practical importance to minimize rejects, to improve the quality of the manufactured cable products, to reduce raw material costs in production, and, consequently, to reduce production costs.

A wide range of instruments and devices of different types has been developed to control geometrical sizes of wires and cables. The existing foreign counterparts of similar devices with good metrological characteristics do not fully meet the production requirements. They have the following disadvantages:

- the complexity of the technical solutions, and a high cost of maintenance and purchase;
- the presence of mechanical moving parts reducing the potential reliability;
- a large size in the longitudinal direction, and some one-piece constructions imposing a restriction on their use.

The need to measure the extrusion die in the output (conductor insulation with the temperature of ~ 130 C) and the continuity of the process does not allow using the contact and destructive methods of eccentricity control. Figure 1 shows the insulated conductor cross-section, where the distance from the center of the cable conductor to the center of the cable sheath (line segment e) is the cable eccentricity, and line segments e_x and e_y are the eccentricity projections along the corresponding axes. The values of these characteristics are to be used for the automatic process control.

The eccentricity measuring technique includes an optical two-dimensional system to determine the position of the center, the diameter of the cable outer sheath, and a transformer mutual inductance magnetic sensor to measure the displacement of the cable conductor center. The data processing of optical and electromagnetic channels makes it possible to determine the eccentricity with sufficient accuracy. Figure 2*b* shows a diagram of the eccentricity measuring instrument, where *W1.1–W1.4* are the coils of the magnetic sensor which measures the displacement of the cable conductor for the first channel, *W2.1–W2.4* are the coils for the second channel, *LAZ1* is a laser and *CCD1* is a radiation detector for the first channel of the optical measuring system, and *LAZ2* and *CCD2* are those for the second channel. The performance of the mutual inductance magnetic sensor measuring the position of the cable conductor is investigated in [1– 3].

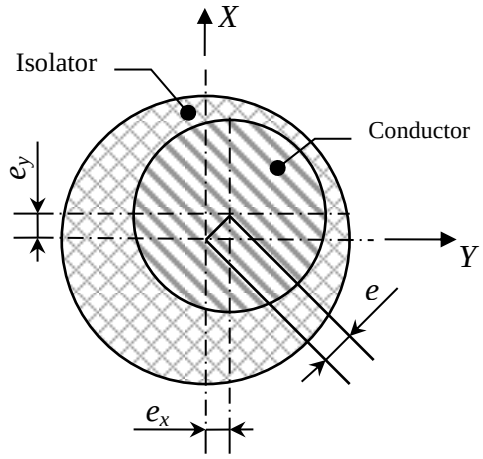

Figure 1. Wire section. Line segment e is the eccentricity under evaluation.

A range of advantages in relation to other optical measuring methods is achieved when the eccentricity and diameter of round wire materials is measured with the help of the laser beam divergence technique [4, 5]. Particularly, the lack of catadioptric optical system and movable optical components essentially simplifies the optical system and design of a primary measuring transducer. Design and production of two-dimensional diameter measuring instruments based on this method, is a promising trend in cable instrument engineering due to their reliability, relative ease of fabrication, and objective adjustment.

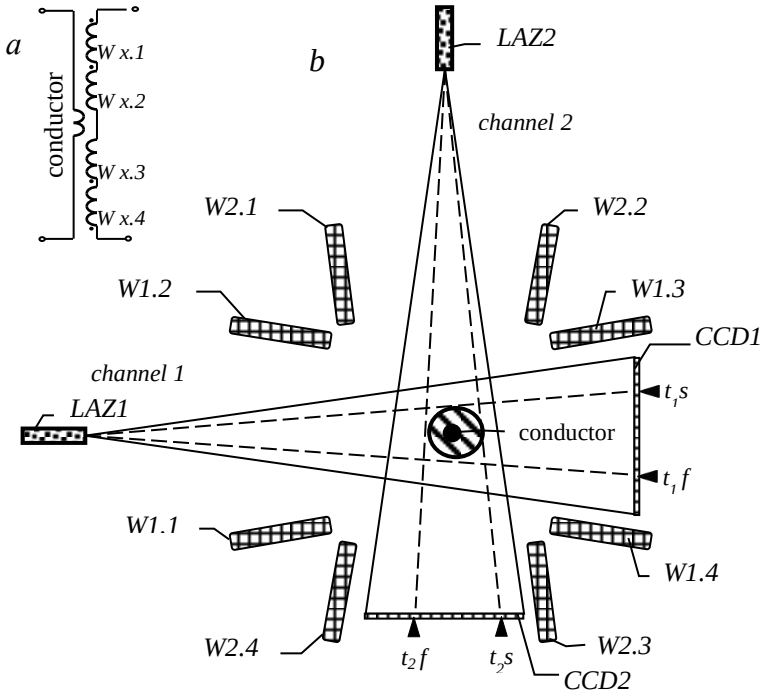

Figure 2. Optical inductive sensor: *a*) connection circuit of the magnetic sensor winding for one of the channels; *b*) the transducer design, where LAZ_1 and $LAZ_2$are point radiation sources; $CCD_1$and CCD_2 are multielement photodetectors for the1st and the 2nd measuring channels, respectively; the quantities t_1f, t_1s *and* t_2f, t_2s are the shadow boundaries of the workpiece under evaluation;*W1.1–W1.4* are coils of the magnetic sensor which measures the displacement of the cable conductor for the first channel, *W2.1–W2.4* are those for the second channel.

Laser beam divergence technique for diameter measurement used for long wire materials is based on detection of shadow boundaries of the object by means of multielement linear photodetectors placed in two orthogonal measuring channels. Figure 2 shows a schematic layout of the optical two-dimensional primary measuring transducer which implements this measurement technique. Traces of laser beams emitted by point radiation sources LAZ_1 and LAZ_2 are shown by dashed lines. These laser beams are directed tangentially to the work piece edges and form light–shadow boundaries t_1f, $t1s$ и t_2f, t_2s on the respective multielement photodetectors CCD_1 and CCD_2. This technique and functions of primary measuring data transformation are described in detail in works [6] and [7].

In practical application, an accurate detection of geometrical boundaries of rising and falling edges of a work piece shadows using a multielement photodetector is rather complicated. This is because the slew rate and the shape of boundaries depend on a local lighting of photodetector and a position of the work piece in a plane orthogonal to the photodetector surface. Scratches, dust, dirt and other during-operation defects of optical glass of measuring instruments affect the accuracy of shadow boundary determination. Even though these defects will be taken into account or effectively eliminated, the accuracy of optical instruments is restricted by diffraction effects occurring at the work piece boundaries that results in a blurring effect of a shadow.

In the patent [8], the principle of the shadow boundary determination is described on the basis of the extreme value distribution from the edge of the opaque object. It is a well-known technique that was investigated in the works [9] and [10]. The principle of the shadow boundary determination is widely used in science and technology [11–22]. In particular, it is applied to enhance the accuracy of geometry measurements of various wire materials. In order to improve a resolution of optical transducers based on a laser beam divergence measurement technique, the analysis of the Fresnel diffraction pattern of large-scale objects was carried out by instruments produced by Sikora and Zumbach Companies. However, in the above mentioned literature, the transformation function allowing the accurate mathematical calculation of the boundary position in measuring wire materials with diameters exceeding the wavelength is not described. This fact restricts the application of Fresnel diffraction by optical transducers based on this technique. In addition to the transformation function, the authors present research into the object movements within the gaging zone affecting the diffraction pattern that is very important for the industrial development of measuring devices.

2. Determination technique of the geometrical boundary of shadow based on diffraction.

As shown in Figure 3, the principle of Fresnel diffraction occurs on the boundary of opaque cylindrical objects. Partially the light penetrates into the shadow region while in the illuminated region it forms the system of diffraction minima and maxima, the difference between them monotonically decreases, and the intensity of light goes to the initial illumination I_0. The distance L between the point source and the multielement photodetector depends on the structural properties of the optical transducer and is constant. The distance y may vary depending on a position of the work piece under control.

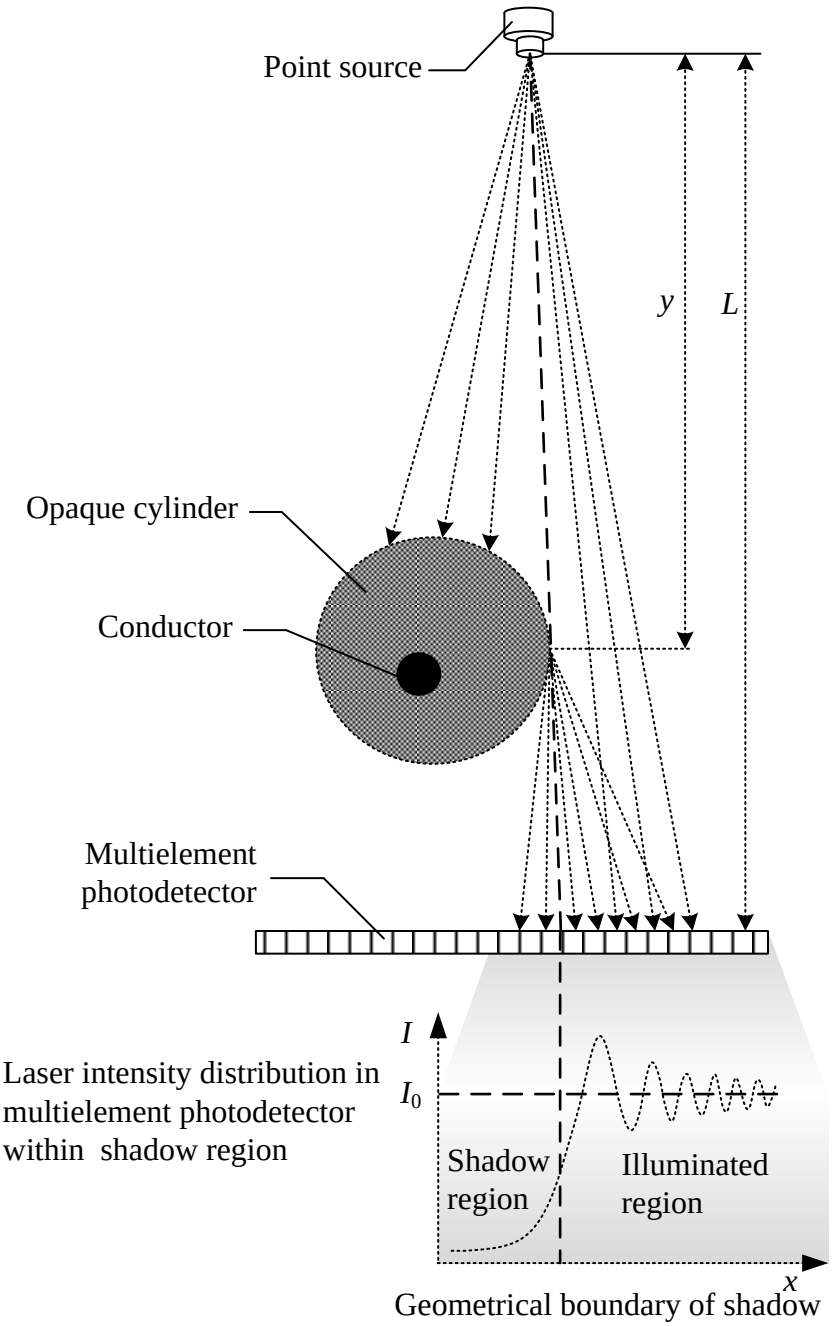

Figure 3. Fresnel diffraction at the boundary of opaque cylinder: I_0–initial illumination; L–distance between the point source and the multielement photodetector; y–distance between the point source and opaque cylinder.

Figure 4 allows the study of diffraction extremum distribution in the vicinity of geometrical boundary. In case the shadow boundary is projected orthogonally to the photodetector plane, the distance X_i from the point X_t to its respective maximum M_i and the distance x_i from the same point X_t to its respective minimum m_i are defined by formulas

$$X_i = \sqrt{\frac{\lambda L(L-y)}{2y}\left(4i+\frac{3}{2}\right)},\ x_i = \sqrt{\frac{\lambda L(L-y)}{2y}\left(4i+\frac{7}{2}\right)}, \quad (1)$$

where i is the number of the respective maximum or minimum starting from zero; λ is the wavelength of the point source (Fig. 3).

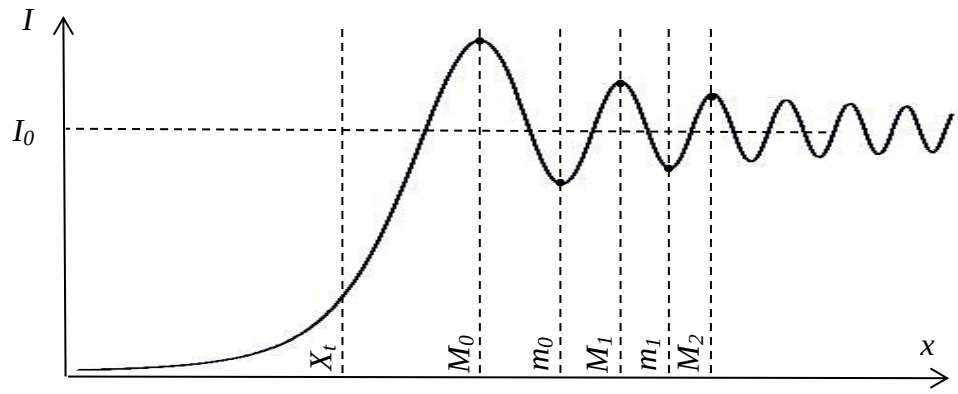

Figure 4.Diffraction extremum distribution in the vicinity of geometrical boundary: X_t– geometrical boundary of shadow; M_0,M_1, M_2–minima of the first, second and third orders respectively; m_0, m_1–minima of the first and second orders respectively.

A position of the boundary X_t on the multielement photodetector is the original value for a calculation of diameter using method presented in [6]. Having determined the distance between the first two maxima (interval M_0M_1) or minima (interval m_0m_1) shown in Figure 4, the boundary X_t can be found. Since factor $\sqrt{\lambda L(L-y)/2y}$ in (1) is fixed for all extreme values, distribution of these values will then be defined by factors $\sqrt{4i+3/2}$ and $\sqrt{4i+7/2}$ for maxima and minima respectively. Thus, the distance between the extreme values can change proportionally depending on parameters of L and y, however, correlation between them is being constant. In particular, the interval X_tM_0 correlates with the interval M_0M_1 with fixed coefficient 1,093, while a correlation between intervals X_tm_0 and m_0m_1 equals to 2,154. Thus, the formulas below can be derived to find coordinates of geometrical boundaries of rising and falling edges:

$$\begin{aligned} X_{ft} &= 1,093(M_0 - M_1) + M_0 = 2,154(m_0 - m_1) + m_0 \\ X_{st} &= M_0 - 1,093(M_1 - M_0) = m_0 - 2,154(m_1 - m_0) \end{aligned}, \quad (2)$$

where X_{ft} and X_{st} are positions of geometrical boundaries of rising and falling edges; M_0, M_1, m_0, m_1 are the extreme values of diffraction distribution.

3. Determination of the shadow boundary position when the object under evaluation is placed in an arbitrary position

The test installation was designed to conduct the experiment. The block diagram of the test installation is shown in Figure 5.

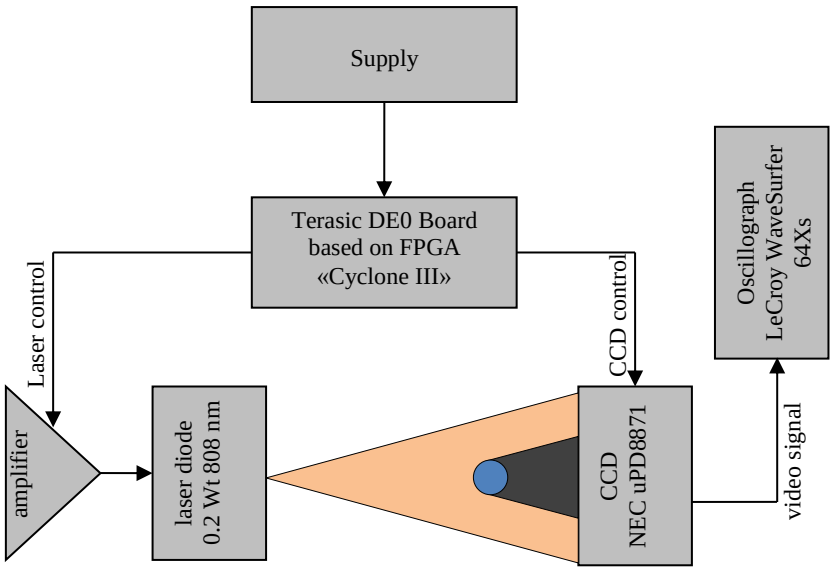

Figure 5. Block diagram of the test installation

The angle measurement was provided by the mechanical dial with 1′angle-error detection. In the centre of the mechanical dial a board with the multielement photodetector was fixed. The cylindrical object~4 mm diameter was also mounted in the centre next to the board. The linear CCD (charge-coupled device) NEC μPD8871 was used as a multielement photodetector. It has 3 rows of 10680 pixels and 4×4 μm photocell size. CCD scanning rate and exposure time were 1 kHz and about 50 ms respectively. Diode laser HLDH-808-B20001 with parameters of 808 nm wave length, 0,2 Wt optical power, and 42ºbeam divergence angle, was fixed on a hanger mounted to the dial. A driving pulse generation for the board with the multielement photodetector and laser emitter was performed by the Terasic DE0 Board based on FPGA Cyclone III. FPGA Cyclone III is used to accurately CCD clock and control with 20 MHz frequency observing all intervals in compliance with its datasheet. Extremum positions for the diffraction pattern were registered by LeCroy WaveSurfer 64Xs Digital Oscilloscope. The test installation was supplied from the power source.

Figure 6 presents the oscillogram of the work piece scanned by a laser beam. All the notations used in this Figure are taken from Figure 4.

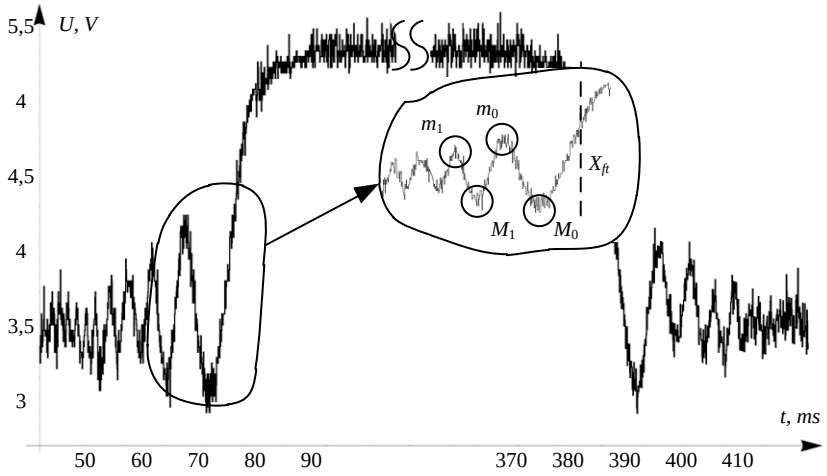

Figure 6. Oscillogram of the work piece with diffraction effects occurred at the boundaries.

Figure 7 describes the experimental dependence between coefficients k_M and k_m (experimentally equal to 2 and 1,1 respectively) and the workpiece movement within the gaging zone normal to the multielement photodetector. As shown in Figure 7, their values are found to be in good agreement with theoretical results. These values are constant within the wide range of the work piece movements that is true for formulas (2) in case when the diffraction pattern is formed by an incident rim ray normal to the surface of multielement photodetector.

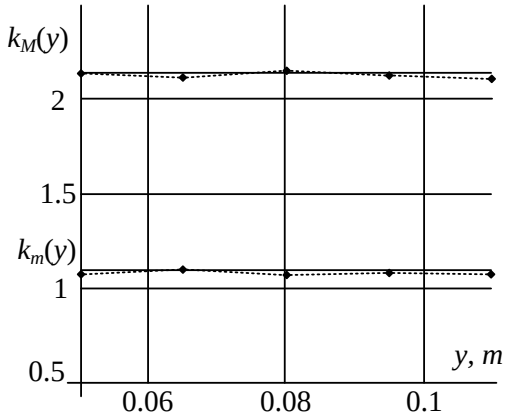

Figure 7. Dependence between scale coefficients of diffraction and the work piece movements within the gaging zone: $k_M(y)$ and $k_m(y)$ – coefficients for the first two maxima respectively.

However, in real instruments a work piece can move not only along the axis normal to the photodetector plane but also in any other direction. This results in the fact that rim rays incident at an angle α different from 90º, and the geometry of the optical system including parameters L and y, is transformed to parameters L' and y'. Diffraction extremum distributionis also transformed from X_t, M_i, m_i to X_t', M_i', m_i' states depending on the incident angle α, where X is the geometrical boundary of shadow; M and m are maxima and minima of the i-th order as shown in Figure 8.

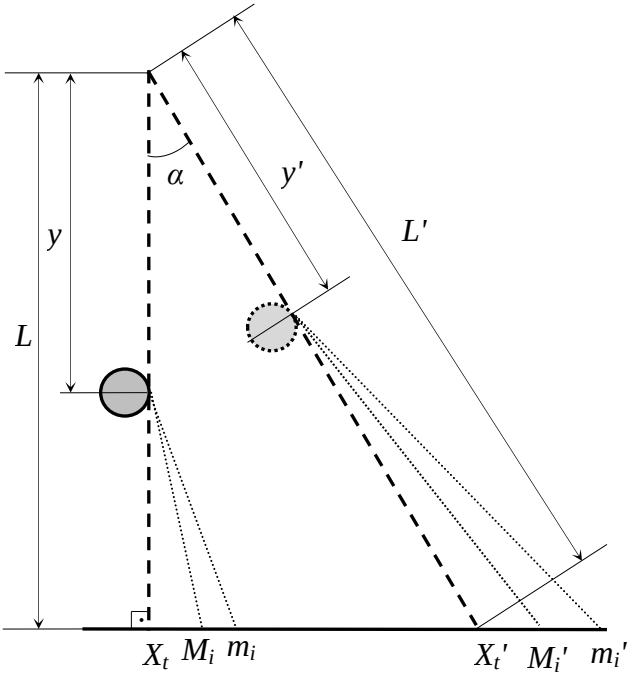

Figure 8. Formation of diffraction pattern on the multielement photodetector at the angle of incidence α.

To validate formulas (2) in case of oblique incidence of rim rays, it is necessary to clarify the manner in which distances between the principle extreme values of the diffraction pattern correlate depending on the angle of incidence. Distances between the first and the second order and between the second and the third order maxima of diffraction pattern were taken as test distances that correspond to intervals M_0M_1 and M_1M_2 shown in Figure 4.

Diagrams shown in Figure 9*a*, demonstrate the empirical relation between intervals M_0M_1 and M_1M_2 and the incident angle α. Zero corresponds to a normal incidence of a rim ray. As it was assumed, distances between the extreme values increase with the increase of beam deflection from the normal to the photodetector plane. As shown in Figure 9*b*, the dependence diagram determines a proportionality of a distance change between these extreme values. This diagram demonstrates how the coefficient $k(\alpha)$affects the correlation M_0M_1/M_1M_2depending on the angle of incidence. Fig. 9, *b* shows that coefficient $k(\alpha)$ (experimentally equal to 1,35) keeps constant under a wide range of incident angle that proves a proportional change of distances between the extreme values of diffraction pattern. This allows formulas (2) to be used for an accurate detection of the geometrical boundary of the work piece shadow in a wide range of its movements.

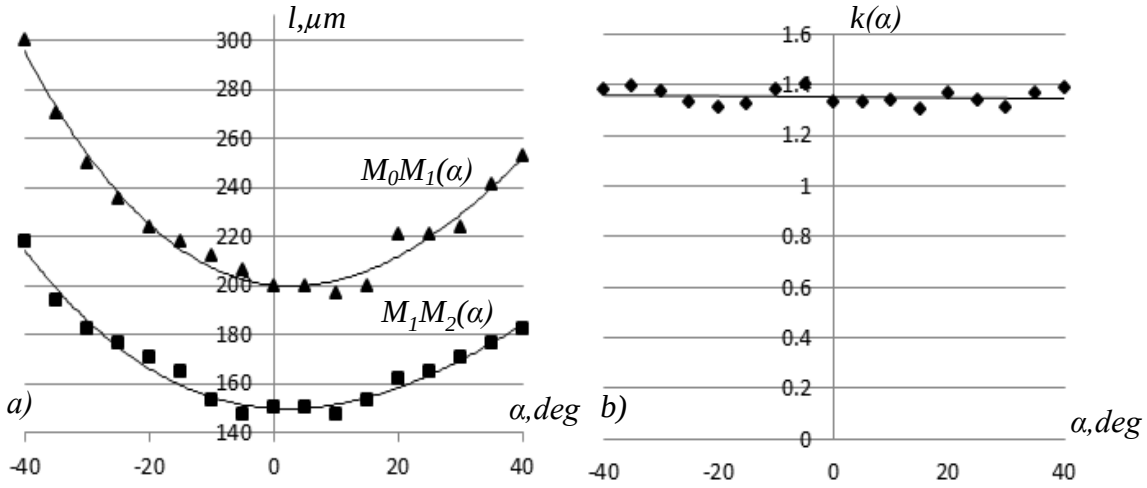

Figure 9.Diffraction extreme values depending on the rim ray angle of incidence: *a)* M_0M_1 and M_1M_2 relation depending on the angle of incidence α; *b)* coefficient k and incident angle α dependence.

4. Discussion

Techniques suggested in this work were tested at various intensities of laser radiation similar to a real operation of a measuring instrument. Results of investigation are given in Table 1 as compared to those obtained for a classical amplitude detector which detects shadow position by the slew rate and the shape of boundaries on the CCD picture.

Table 1 Comparison of detectors

I	Amplitude detector		Diffraction detector	
	Rising and falling edges (pixel)	Detection error (μm)	Rising and falling edges (pixel)	Detection error (μm)
$0.95 \cdot I_0$	1875.2	-10.4	1876.7	-0.4
I_0	1877.8	0	1876.8	0
$1.05 \cdot I_0$	1880.7	+11.6	1877.0	+0.8

The detection error for the shadow boundary as shown in Figure 6, comes to 10 μm at laser brightness variation ±5% from a certain initial value $I_{0.}$ During operation, this error can increase multiply due to contamination of optical elements, detection errors of rising and falling edges being

summed up for the diameter calculation. In suggested technique of the boundary detection (by diffraction pattern extreme values) the error is around 1 μm at the similar flare brightness. This provides high metrological characteristics of measuring instruments regardless of the optic emitter drift characteristics and purity of optics instruments.

Suggested techniques were approved on many opaque cylindrical objects with diameters ranging from 0,5 to 40 mm and made of different materials such as polypropylene, polyethylene, polyvinylchloride, rubber, metals, etc. Semiconductor diodes 808 nm length and 0,2-0,5 Wt energy were used in this study. As a rule, they possess different beam divergence along different symmetry planes, in particular $\Theta// \approx 8 \div 11^{\circ}$, $\Theta\perp \approx 39 \div 48^{\circ}$. In laser beam divergence technique for diameter measurement, only semiplane $\Theta\perp$ is used to provide a flare of the entire gaging zone. Therefore, other laser positions and, consequently, differences in the light beam polarization are not presented in this paper.

Depending on a configuration of the optical system, suggested techniques provide resolution for a single diameter measurement within 2÷3 μm range allowing for optical magnification of a laser-beam-divergence optical transducer (Fig. 2). Further mathematical processing of obtained data in conformance with methodology described in works [6, 7]. In the work [23] there are also considered statistical methods for increasing of resolution up to 1 μm for optical measuring devices applied to control cylindrical extended objects such as cables, wires, cords etc.

5. Conclusions

The paper shows the technique of measuring the diameter on the basis of light diffraction at the object boundary. The expression (2) to determine the exact position of the shadow geometric boundary of the object without the amplitude analysis of the image front has been obtained. The conversion functions allow determination of the shadow boundary regardless of the spatial position of the object under evaluation. The obtained results enable a precise control of the inner diameter of extended objects and eccentricity of a single cable if the described optical transducer is used together with the inductive transducer investigated in [1–3].

REFERENCES

[1] Goldshtein A.E. and Fedorov E.M. A Mutually Inductive Measuring Transducer of Transverse Displacements of a Rectilinear Conductor *Russian journal of nondestructive testing* Vol. 46 **6** 2010.

[2] Patent RF № 2010107490/28; pending 01.03.10; published 27.06.11, bulletin № 18, «Induktivno-opticheskij preobrazovatel' izmeritelja jekscentrichnosti jelektricheskogo kabelja» / A. E. Gol'dshtejn, V. V. Red'ko, E. M. Fedorov; Tomskij politehnicheskij universitet (TPU); Nauchno-proizvodstvennoe ob'edinenie "Redvill".

[3] Fedorov E.M., Gol'dshtejn A.E., Svendrovskij A.R., Red'ko V.V. «Izmeritel' diametra i jekscentrichnosti jelektricheskogo kabelja na osnove induktivnoopticheskogo metoda» *Izvestija* TPU 2010 **2**

[4] C.J Tay, S.L Toh, H.M Shang Time delay and integration imaging for internal profile inspection, *Optics & Laser Technology*, Volume 30 *8* 1998, Pp. 459–465

[5] Jinhui Lan, Jian Li, Guangda Hu, Yiliang Zeng Distance estimation using a panoramic sensor based on a novel spherical optical flow algorithm, *Optics & Laser Technology*, Volume 45, 2013, Pp.168–176

[6] Svendrovskii A.R., Raschet diametra v beskontaktnykh dvukhkoordinatnykh izmeritelyakh [Measurement of diameter by non-contact two-dimensional detectors]. Proc. 1stAll-Rus. Sci. Conf. 'Scientific and engineering problems of instrument engineering'. Tomsk, 2005. Pp. 31–33. (rus)

[7] Fedorov E.M., Edlichko A.A. Vychislenie geometricheskikh parametrov dvukhkoordinatnykh izmeritelei diametra protyazhennykh izdelii [Calculation of geometrical parameters of two-dimensional instruments used for measuring diameter of long wire materials] *Bulletin of the Tomsk Polytechnic University*, 2008. No. 2. (rus)
[8] Patent N EP 0924493 B1 «Measurement of diameter using diffraction borders and electronic soiling correction». Adrian Beining, Werner Dr.-Ing. Blohm, HaraldSikora, 2002.
[9] Sommerfeld A., Optics (German edition 1950, English translation: Academic Press, 1964), sec 37, 38.
[10] Born and E. Wolf, Principles of Optics, 3rd Edition Pergamon Press, 1965.
[11] Toenshoff, H. K., Tuennermann, A., Korthals, J., SPIE, Use of Fresnel diffraction for the measurement of rotational symmetrical workpieces. Proceedings SPIE The International Society For Optical Engineering, 3784, 1999, Pp. 334-343.
[12] Chi-Tang Li, James V. Tietz, Improved accuracy of the laser diffraction technique for diameter measurement of small fibres. *Journal of Materials Science*, 1990, Volume 25 **11** Pp. 4694-4698.
[13] Khodier S.A., Measurement of wire diameter by optical diffraction. Original Research Article Optics & Laser Technology, Volume 36, **1**, 2004, Pp. 63–67.
[14] Durgin G.D. , The Practical Behavior of Various Edge-Diffraction Formulas. *IEEE Antennas and Propagation Magazine*, Volume 51, **3**, 2009, Pp. 24–35.
[15] George S., Straight edge diffraction using a laser. *Physics Education*, Volume 7, **6**, 1972, Pp. 349–352
[16] Jinhuan Li, Osami Sasaki, and Takamasa Suzuki, Measurement of diameter of metal cylinders using a sinusoidally vibrating interference pattern. Optics Communications, Volume 260, Issue 2, 2006, Pp. 398-402.
[17] R. Jabłoński, J. Mąkowski Measurement of cylinder diameter by laser scanning, Recent Advances in Mechatronics 2007, pp 596-600
[18] Y. Chugui,V. Bazin,L. Finogenov,S. Makarov,A. Verkhogliad Optical electronic measuring systems and laser technologies for scientific and industrial applications, International Symposium on Instrumentation and Control Technology No6, Beijing , CHINE (2006) 2006 , vol. 6357 (2)[Note(s) : 2 vol.,] (13 ref.) **ISBN 0-8194-6452-X** ; 978-0-8194-6452-1
[19] Ryszard Jablonski, Pawel Fotowicz New generation of laser mike, *Proc. SPIE 4420, Laser Metrology for Precision Measurement and Inspection in Industry*, 91 (September 11, 2001); doi:10.1117/12.439198
[20] Smith S.W. "Chapter 8: The Discrete Fourier Transform". The Scientist and Engineer's Guide to Digital Signal Processing (Second ed.). San Diego, Calif.: California Technical Publishing. **ISBN 0-9660176-3-3.1999.**
[21] Luis Miguel Sanchez-Brea, Juan Carlos Martinez-Anton, Eusebio Bernabeu Effect of the refraction index in the diameter estimation of thin metallic wires, *Proc. SPIE 5858, Nano- and Micro-Metrology*, 585819 (August 26, 2005); doi:10.1117/12.612652
[22] Lars Benckert, Lars Forsberg, and Nils-Erik Molin, Fresnel diffraction of a Gaussian laser beam by polished metal cylinders, *Applied Optics*, Vol. 29, **3**, pp. 416-421 (1990)
[23] Yury A. Chursin, Evgeny M. Fedorov "Methods of resolution enhancement of laser diameter measuring instruments" *Optics & Laser Technology*, Volume 67, 2015, Pages 86-92